Contents lists available at ScienceDirect

Harmful Algae

journal homepage: www.elsevier.com/locate/hal





Alexandrium on the Alaskan Beaufort Sea shelf: Impact of upwelling in a warming Arctic

Sveinn V. Einarsson ^{a,1}, Kate E. Lowry ^{b,c}, Peigen Lin ^c, Robert S. Pickart ^c, Carin J. Ashjian ^c, P. Dreux Chappell ^{a,*}

- ^a Department of Ocean and Earth Sciences, Old Dominion University, Norfolk, VA, USA
- b Science Philanthropy Alliance, Palo Alto, CA, USA
- ^c Woods Hole Oceanographic Institution, Woods Hole, MA, USA

ARTICLE INFO

Edited by Dr. C. Gobler

Keywords: Alexandrium catenella Beaufort Sea Upwelling Shelfbreak jet Saxitoxin Arctic

ABSTRACT

The harmful algal genus Alexandrium has characteristically been found in temperate and subtropical regions; however recent evidence suggests global warming may be expanding its range into high latitude waters. Alexandrium cysts have previously been documented in the Chukchi Sea and we hypothesize that Alexandrium may be expanding further into the Arctic due to distribution by the Beaufort shelfbreak jet. Here we document the presence of Alexandrium catenella along the Alaskan Beaufort Sea shelf, marking an expansion of its known range. The observations of A. catenella were made using three different methods: FlowCAM imaging, 18S eukaryotic sequencing, and real-time quantitative PCR. Four occupations of a shelf/slope transect spanned the evolution of a strong wind-driven upwelling event over a 5-day period. A nearby mooring provided the physical context for the event, revealing that enhanced easterly winds reversed the Beaufort shelfbreak jet to the west and induced upwelling of colder, denser water onto the outer shelf. A. catenella sequences dominated the surface phytoplankton community at the onset of the upwelling event. This signal vanished during and after the event, likely due to a combination of alongstream advection, cross-stream advection, and wind mixing. These results suggest contrasting physical processes that are both subject to global warming amplification, delivery of warm waters via the Beaufort shelfbreak jet and upwelling, may control the proliferation of this potential harmful alga into the Arctic.

1. Introduction

Harmful algal blooms (HABs) have become an increasingly important issue for public health. Although a recent study concluded that it was additional monitoring and awareness rather than a global increase in HABs that led to more documented instances of HABs and related illnesses such as paralytic shellfish poisoning (PSP) from 1985 to 2018 (Hallegraeff et al., 2021), there is evidence for both local and regional changes amongst certain HABs, including expansion of PSP into new regions associated with ocean warming (Anderson et al., 2021b). The majority of human health problems associated with HABs come from the consumption of shellfish (Grattan et al., 2016) with PSP accounting for a third of the shellfish illnesses (Hallegraeff et al., 2021). PSP can occur when a neurotoxin, such as saxitoxin, is bioaccumulated through filter feeders and fish (Cusick and Sayler, 2013; Wang, 2008), and is

subsequently consumed. Certain species of dinoflagellates are associated with saxitoxin production and PSP outbreaks, making them a consistent concern for public health and coastal ecosystem services (Grattan et al., 2016; Hallegraeff et al., 2021). The Alexandrium genus is one of the dinoflagellate genera that has been found to be the causative agent of many instances of shellfish poisoning along the coastal United States (Anderson et al., 2008, 2021b; Lewitus et al., 2012). The species Alexandrium catenella, which is a well-studied member of the genus known for its ability to produce saxitoxin and causing PSP outbreaks (John et al., 2014), is of particular focus for this study due to recent documented expansion into the Arctic Ocean (Anderson et al., 2021a). While the Alexandrium genus is now a globally abundant dinoflagellate, until 1970, the Alexandrium tamarense species complex (which includes A. catenella) was only found in Europe, North America, and Japan – although it is still characteristically found in temperate and subtropical

E-mail address: pdchappe@odu.edu (P.D. Chappell).

 $^{^{\}star}$ Corresponding author.

Present address: University of Florida Dept Microbiology and Cell Science, USDA ARS affiliate, Gainesville, FL, USA

regions (Lilly et al., 2007). It is important to note that the accepted nomenclature of the *A. tamarense* species complex was recently changed to: Group 1: *A. catenella*, Group 2: *A. mediterraneum*, Group 3: *A. tamarense*, Group 4: *A. pacificum*, and Group 5: *A. austaliense* (Fraga et al., 2015; John et al., 2014; Prud'homme van Reine, 2017). As prior studies have used older nomenclature customs, clarification is provided throughout this manuscript where appropriate.

The Arctic Ocean has been warming faster than any other place on Earth, resulting in more extensive sea ice retreat each year (Holland and Bitz, 2003; Manabe and Stouffer, 1980). It is predicted that the Arctic will continue to warm because of enhanced ocean current heat transport (Marshall et al., 2014, 2015) combined with Arctic amplification (Kim et al., 2016). Heat transport through the Bering Strait has increased significantly over the past three decades (Woodgate, 2018) and is forecast to be one of the most influential continued imports of heat to the Arctic (van der Linden et al., 2019). The inflow through the Bering Strait is of particular interest to this study because it brings Pacific summer water to the Alaskan Beaufort Sea shelf. This warm water is advected into the Alaskan Beaufort Sea via the Alaskan Coastal Current which, upon exiting Barrow Canyon, forms the eastward-flowing Beaufort shelfbreak jet (Nikolopoulos et al., 2009) (Fig 1). Increased heat transport in this region associated with the Beaufort shelfbreak jet has the potential to expand the domain of normally temperate algae into the Arctic. Of the temperate algae, expansion of Alexandrium further into the Arctic is of particular concern as this expansion could have deleterious implications for the economy and food production in remote regions of Alaska. Prior evidence of negative impacts have been documented in marine mammal beaching along the Alaskan coast up to Point Barrow that was associated with the presence of the *Alexandrium* toxin saxitoxin (Lefebvre et al., 2016). Cyst beds of saxitoxin producing species of Alexandrium have also been documented as far north as the Bering Sea and Chukchi Sea (Natsuike et al., 2017a, 2013) and most recently seen ~100 km west of our study site in the Alaskan Beaufort Sea (Anderson et al., 2021a). In addition to warming inflow into the Arctic resulting in evidence of Alexandrium expansion (Anderson et al., 2021a; Natsuike et al., 2017a), average temperatures suitable for germination and growth of Alexandrium (5-15 °C, (Natsuike et al., 2017b)) have been observed just west of our study area in a region where A. catenella cyst beds have recently been documented (Anderson et al., 2021a).

While the Beaufort shelfbreak jet may be delivering temperate algae further into the Arctic, once delivered into the region phytoplankton may be influenced by other complicating physical process such as wind-driven upwelling. Specifically, under intensified easterly winds the Beaufort shelfbreak jet reverses to the west, followed shortly thereafter

by upwelling (Pickart et al., 2009). This upwelling can deliver nutrient-rich Pacific-origin winter water from the Arctic basin onto the shelf (Lin et al., 2019; Pickart et al., 2011). Upwelling in the Beaufort Sea is predicted to increase in strength and occurrence as a result of a warming climate (Pickart et al., 2013). The upwelled nutrient-rich cold water can reach the surface euphotic zone where phytoplankton and other biota have access to it, often leading to a bloom of phytoplankton and subsequently to an increase in upper trophic level biomass in the Alaskan Beaufort Sea (Ashjian et al., 2010). Some phytoplankton respond better than others to water column turbulence and increased nutrient concentrations that are associated with upwelling events. Diatoms, for example, are unicellular eukaryotic phytoplankton known to grow faster than other phytoplankton in response to nutrient pulses, allowing them to bloom in upwelling environments (Biller et al., 2013). By contrast, dinoflagellates are generally more suited to bloom when the upper water column is stratified, such as after upwelling events when wind mixing ceases (Lewitus et al., 2012). As a result of this dynamic, when upwelling begins it is common for the phytoplankton community to shift to diatoms, and, when upwelling relaxes, the environment becomes more favorable to dinoflagellates and diatom growth often enters a lag phase (Smayda and Trainer, 2010).

Motivated by a desire to explore how these two competing physical factors, warm water intrusion via the Beaufort shelfbreak jet and upwelling, may be influencing Alexandrium populations in the coastal Arctic, this study uses multiple methods to evaluate Alexandrium in the Beaufort shelf region at the onset, during, and after an upwelling event. We hypothesize that the Beaufort shelfbreak jet is transporting warm water suitable for Alexandrium growth and expanding its habitable region. We further hypothesize that increased upwelling can mitigate this expansion of Alexandrium by displacing these warmer waters in addition to increasing turbulence. Using data from a FlowCam imaging system, we show evidence of Alexandrium further into the eastern Pacific Arctic domain than has been previously observed. The species of Alexandrium was subsequently determined to be A. catenella using both an 18S rRNA sequencing method and a 28S rRNA real-time quantitative PCR method. As A. catenella is a toxin producing species, this proliferation is of particular concern and further study of toxicity of A. catenella in this region may be warranted.

2. Material and methods

2.1. Physical data collection

A research cruise on R/V Sikuliaq took place in August-September

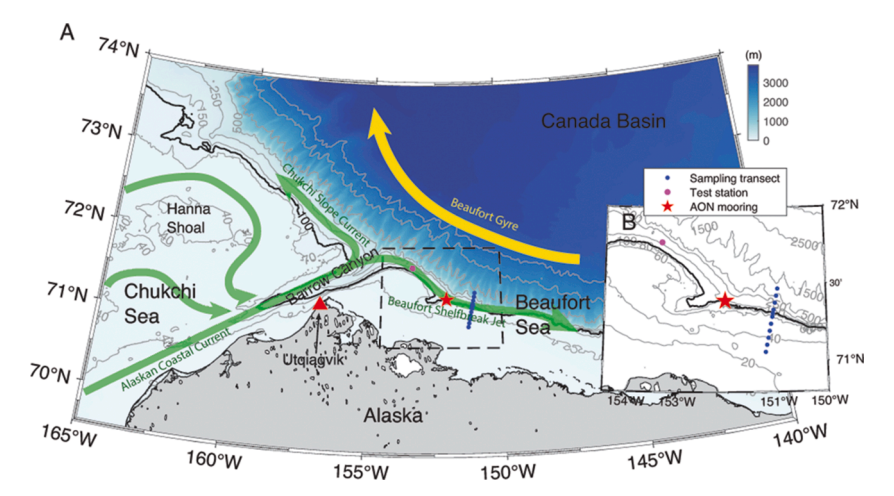


Fig. 1. Map of the study area, including place names, and schematic circulation of the region. The flow emanating from Barrow Canyon splits, with the eastward-flowing portion forming the Beaufort Shelfbreak Jet. The locations of the repeat transect, the AON mooring, and the test station are marked (see the legend). The bathymetry is from IBCAO v3. The inset shows an enlarged view of the measurement sites used in the study.

Harmful Algae 120 (2022) 102346

2017 as part of a program investigating upwelling in the western Beaufort Sea. During the cruise, a shelf-slope transect near 151°W was occupied four times between 30 August and 5 September (Fig. 1). An additional test station was sampled at 71.77°N 153.34°W and is included here. Conductivity-temperature-depth (CTD) stations were carried out using a Sea-Bird Electronics SBE 911-plus (Bellevue, WA, USA) with dual temperature and conductivity sensors, as well as a dissolved oxygen sensor (Sea-Bird SBE43) and a fluorometer (Wetlabs FLRTD). The stations were spaced ≤5 km apart, and each occupation of the transect took between 10 and 18 h to complete. The transect was located near a long-term mooring deployed as part of the Arctic Observing Network (AON) (Lin et al., 2019). The mooring is situated at the 147 m isobath in the core of the Beaufort shelfbreak jet, roughly 35 km west of the transect (Fig. 1). Velocity was measured hourly from the mooring throughout the Sikuliag cruise using an upward-facing Nortek Signature 250 kHz acoustic Doppler current profiler (ADCP) with 4 m bins, and temperature and conductivity (salinity) were measured hourly using 8 SBE MicroCATs (Sea-Bird) spaced through the water column from 33 m to near the seafloor. Wind data at 9.4 m height were obtained from the meteorological station in Utqiagvik, AK (Fig. 1), and 10-m wind and sea-level pressure fields from the ERA5 reanalysis (Hersbach et al., 2018) were used as well. We consider the alongcoast wind (105°T, positive out of west), and the alongstream velocity (125°T, positive to the east) (Lin et al., 2019; Nikolopoulos et al., 2009).

2.2. Sample collection

Near-surface water and water from the depth of the chlorophyll a maximum were collected using Niskin bottles on the CTD rosette. Up to 4 L of seawater were drawn into 10% HCl acid-cleaned and seawaterrinsed Nalgene bottles (ThermoFisher Scientific; Waltham, MA, USA), then subsequently filtered through a 0.22 μm Sterivex filter (Millipore Sigma, Merck KGaA; Darmstadt, Germany) using a peristaltic pump. Filters were immediately frozen at -80 °C until DNA extraction. Seawater was also pre-filtered through a 100 µm Nitex mesh, and 5 mL of filtered seawater was run at 40x (300 μ m) and 100x (100 μ m) magnification on the FlowCAM (Yokogawa Fluid Imaging Technologies; Scarborough, ME, USA). Nitrate profiles were collected at 7 to 10 stations per transect occupation with an optical nitrate sensor (SUNA V2, Sea-Bird) powered with an external 51 Ah battery pack. To create depth profiles, we aligned the SUNA and CTD data by recorded time. Water samples from 4 to 6 depths at 12 stations selected from the broader cruise sampling efforts, which also included additional transects along the Beaufort Sea shelf not presented here, were taken for direct nitrate concentration measurements to calibrate the nitrate sensor. Nitrate concentrations in those water samples were measured using an Alpkem RFA continuous flow analyzer following standard colorimetric protocols (Gordon et al., 1993). SUNA nitrate profiles were calibrated by fitting a linear regression to direct measurements from corresponding depths. While additional nutrients including phosphate and silicic acid were measured from the broader cruise samples used to calibrate the SUNA sensor, only a few of the stations from this manuscript were part of the calibration set. Because of this, only calibrated SUNA nitrate data are presented here.

2.3. DNA extraction

An ethanol cleaned PVC pipe cutter was used to open the 0.22 μm Sterivex (Millipore Sigma) filters and an autoclaved scalpel used to remove the filter. Each filter was added to a 2 mL tube containing AP1 Buffer (Qiagen; Hilden, Germany) and silicon beads of 0.1- and 0.5-mm size. Bead beating was done using a bead beating attachment on a Vortex-Genie® 2 and vortexing at maximum speed (3200 RPM) for $\sim\!\!2$ min and DNA was extracted using the DNeasy Plant Mini Kit (Qiagen) following the manufacturer's protocol.

2.4. DNA amplification and sequencing analysis

To analyze for eukaryotic community composition, the SSU rRNA 18S V9 marker gene was amplified from DNA by PCR in triplicate using 1x master mix (Phusion HF Mastermix, ThermoFisher) and primers used in the Earth Microbiome Project's standard 18S Illumina Sequencing protocol (Stoeck et al., 2010) on a SimpliAmp thermal cycler (Applied Biosystems; Waltham, MA, USA). Triplicate PCR products were pooled, and the amplified DNA was purified using Mag-Beads (AMPure XP, Beckman Coulter; Indianapolis, Indiana, USA). The amplified DNA was then subject to another round of PCR, to attach MiSeq indices (Illumina; San Diego, CA, USA), and Mag-Bead purified again. Sequencing was done using the Illumina MiSeq Desktop Sequencer at Old Dominion University (Norfolk, Virginia, USA) using a 2 × 300-bp kit. Sequences were analyzed by pipeline analysis using DADA2 (Callahan et al., 2016), with minor exceptions to the default analysis. Reads without primer sequences were discarded from analysis while intact sequences had primers removed using cutadapt (Martin 2011). Average reads per sample were 66,000, and Amplicon Sequence Variants (ASVs) were identified using the BLASTN (Altschul et al., 1990) algorithm to an in-house database including 18S rRNA eukaryote sequences from the National Center for Biotechnology and Information (NCBI; Bethesda, MD, USA) and eukaryotic sequences from SILVA (the German Network for Bioinformatics Infrastructure; Bremen, Germany). To calculate the 18S rRNA A. catenella relative abundance of phytoplankton, the read counts for 4 ASVs for A. catenella (>99% similar) were combined and divided by the combined read counts for to all 18S rRNA phytoplankton hits (which includes ASVs classified as diatoms, dinoflagellates, and haptophytes). We chose to calculate relative abundance of A. catenella in acknowledgement of the compositional nature of high-throughput amplicon sequencing datasets (Gloor et al., 2017).

2.5. qPCR assay

Quantification of the dinoflagellates *A. catenella* and *Alexandrium pacificum* was done in triplicate on a StepOne Plus real-time PCR system (ThermoFisher) using the species specific 28S rRNA qPCR assays of Hosoi-Tanabe and Sako (2005) with 1x TaqMan Fast Advanced Master Mix (ThermoFisher). We note that Hosoi-Tanabe and Sako used the older nomenclature and refer to *A. catenella* as *A. tamarense* and *A. pacificum* as *A. catenella*. Absolute 28S rRNA gene quantification was done using standard curves created by serial dilution of synthetic plasmids (GENEWIZ; South Plainfield, NJ, USA) for both *A. pacificum* (previously *A. catenella*) and *A. catenella* (previously *A. tamarense*) although *A. pacificum* was never detected in our samples and will not be discussed further. *A. catenella* qPCR efficiency was 89% and standards ranged from 55 to 5.5E8 gc/µl.

2.6. Statistical analysis

Significant difference between groups of samples was determined using a Kruskal-Wallis (Kruskal and Wallis, 1952) test. This was done by comparing grouped samples collected on the shelf (excluding station 2.2) at the surface and chl-a depths for the 4 occupations, the onset (A), during (B), and after (C, D) upwelling. The Kruskal-Wallis test was chosen due to a few samples being below detection limit, causing group sample counts to be uneven, and the non-normal distribution of residuals for the one-way ANOVA. Significant differences between individual groups was done using Dunn's post hoc test. Significance is reported with a p-value below the α criterion of 0.05. A linear regression analysis was used to compare log transformed A. catenella 18S rRNA relative sequence abundance and 28S rRNA absolute sequence abundance. This correlation was checked to determine if the changes in absolute and relative abundance of A. catenella corroborated each other to support our argument that A. catenella sequence abundance was higher before upwelling. Additionally, a linear regression analysis compared

the log transformed A. catenella 28S rRNA sequence abundance and CTD fluorescence when A. catenella 18S rRNA sequences accounted for more than 5% of the relative phytoplankton 18S rRNA sequences. This analysis was done to compare fluorescence, absolute and relative sequence abundance to add support to the argument that A. catenella was a primary phytoplankton in the community before upwelling. Strength of relationship is reported as ρ and significance is reported with a p-value below the α criterion of 0.05.

3. Results

3.1. Hydrography

The transect was occupied four times (A, B, C, D) at different stages of a wind-driven upwelling event and the physical context for the event is provided by the meteorological information together with the AON mooring data (Fig. 2). Alongcoast wind velocity from ERA5 and the Utqiagvik weather station is shown in the top panel (Fig. 2A). Water column alongstream velocity, salinity, and potential temperature and density (referenced to the sea surface) are shown in subsequent panels (Fig. 2B-D), covering the full progression of the upwelling event. As the first transect was occupied, the alongcoast winds became upwelling favorable. Subsequent to this, the salinity in the lower part of the water column increased and the Beaufort shelfbreak jet reversed to the west. The second transect was carried out shortly after the peak of the event, while the third occupation occurred after the upwelling had subsided and the eastward-flowing Beaufort shelfbreak jet had become reestablished. The fourth occupation took place as a second, considerably weaker, upwelling event commenced.

The evolution of the large-scale wind and sea-level pressure (SLP) field is shown in Suppl. Fig. 1. Before the first upwelling event, the winds were northerly in the study region associated with the eastern side of the atmospheric Beaufort High. During the upwelling event, the Beaufort High had weakened, but a low-pressure system over Alaska led to a strong zonal SLP gradient over the southern Beaufort Sea. After the event, high SLP was established over Alaska weakening the zonal gradient in the study region, resulting in light easterly winds.

The vertical sections of temperature and density (Fig. 3) and nitrate (Suppl. Fig. 2) of the sampled transects reveal differences throughout the water column between the onset of the primary upwelling event and the subsequent three occupations during/after the event that generally agree with AON mooring data.

3.2. Alexandrium catenella assessment

FlowCAM samples taken during occupation A at the onset of upwelling imaged relatively high levels of *Alexandrium* on the Beaufort Sea shelf Suppl. Table 1, Suppl. Fig. 4) and coincided with the highest absolute and relative gene abundances (Fig. 3, Suppl. Table 1, Suppl. Fig. 4). Based on the absolute 28S rRNA gene abundances of *A. catenella* along with the ratio of *A. catenella* 18S rRNA sequences to total 18S rRNA eukaryotic phytoplankton sequences (diatoms, dinoflagellates, haptophytes), the threshold for being imaged by the FlowCAM was an absolute 28S rRNA gene abundance of $> 3.92E+09~\rm gc~L^{-1}$ and a relative *A. catenella* 18S rRNA abundance of the total phytoplankton community of > 45% (Suppl. Table 1).

Grouping by occupation and averaging the surface and chl-a max samples, the 28S rRNA absolute gene abundance were found to be significantly different using a Kruskal-Wallis test (F=14.65, p=0.0021). Dunn's post hoc test comparing the groups individually (Table 1) found occupation A to be significantly different than occupations B, C, and D while no significant difference was seen between occupations B, C, and D. The same pattern of results was seen with the relative abundance of A. catenella, where a significant difference was found between the occupations (F=18.57, p=0.0003). The only difference being that between occupations B and D there was a significant

difference (Table 2).

The 18S rRNA relative abundance of *A. catenella* sequencing reads to phytoplankton sequencing reads is plotted against the absolute 28S rRNA gene abundance of *A. catenella* (gc L $^{-1}$) with both on a log scale (Fig. 4A). A linear regression showed a significant correlation ($r^2 = 0.87$, p < 0.0001) between absolute gene abundance and relative abundance of *A. catenella*. The relationship between absolute 28S rRNA gene abundance of *A. catenella* (when *A. catenella* was above 5% of the relative 18S rRNA phytoplankton community) and fluorescence (mg m $^{-3}$) measured by the CTD (Fig. 4B) also showed a significant correlation ($r^2 = 0.75$, p-value = 0.0006). When the *A. catenella* was below 5% of the 18S rRNA phytoplankton community, no such relationship exists, suggesting that *A. catenella* was likely a primary phytoplankton in the community before upwelling. Absolute gene abundance of *A. pacificum* was not found in any of the samples and consequently is not included in Supplemental Table 1 or discussed further.

4. Discussion

4.1. Hydrographic context of upwelling/relaxation states during sampling

The study analyzed A. catenella abundances through four stages of upwelling at the same location. As earlier studies have demonstrated that the alongcoast winds are most effective at driving upwelling (Nikolopoulos et al., 2009), we use that metric and data from a AON mooring to provide context for our transect sampling. Prior to the first occupation (A), the alongcoast winds were weakly out of the west, and the Beaufort shelfbreak jet was flowing eastward. As the first section was being occupied, the winds were building out of the east and the Beaufort shelfbreak jet was in the process of reversing. Typically upwelling commences roughly half a day after the Beaufort shelfbreak jet reverses (Pickart et al., 2009), but in this case the upwelling was beginning at the same time as the flow switched directions, as indicated by the uplifting of the isopycnals. The reason for this may be that a strong upwelling event in the region took place from 27 to 29 August (not shown), and the isopycnals had not fully relaxed prior to the main upwelling event considered here. As such, we refer to the first occupation as "onset of upwelling."

The second occupation (B) took place roughly a day after the peak easterly winds, at which point the isopycnals were close to their maximum elevation but beginning to relax. The upper part (shallower than 80 m) of the Beaufort shelfbreak jet remained reversed, while the deeper part was starting to become re-established to the east, which is the typical sequence (Lin et al., 2019). This crossing is referred to as "during upwelling." The third occupation (C) occurred when the bulk of the Beaufort shelfbreak jet was again flowing eastward and the denser isopycnals had descended significantly deeper, which corresponds to "after upwelling." The final occupation (D) of the section was done during the start of another upwelling event that was considerably shorter and weaker. When considered in the context of the primary event, this occupation is also referred to as "after upwelling."

The profile data from our transects revealed that, as the event was beginning and the Beaufort shelfbreak jet was switching directions (occupation A), weakly stratified warm water was present over the outer shelf. This consisted mainly of Alaskan Coastal Water (>4 °C) with a layer of sea-ice melt water occupying the top 10 m. Seaward of the shelf, the cold halocline, centered at the 26.5 kg m $^{-3}$ isopycnal, was at its deepest depth of the four transect occupations. By contrast, during the next three occupations the warm water on the shelf was largely displaced. In particular, the signature of Alaskan Coastal Water nearly disappeared at the surface, replaced by a thicker layer of sea-ice melt water (roughly 25 m thick) and a deep layer of colder, denser Bering Summer Water along the bottom of the outer shelf. The stratification in the upper 50 m became enhanced, which is consistent with past mooring results (Lin et al., 2019). Furthermore, seaward of the shelf the halocline shoaled and became colder. We note, however, that the denser 27.0 and

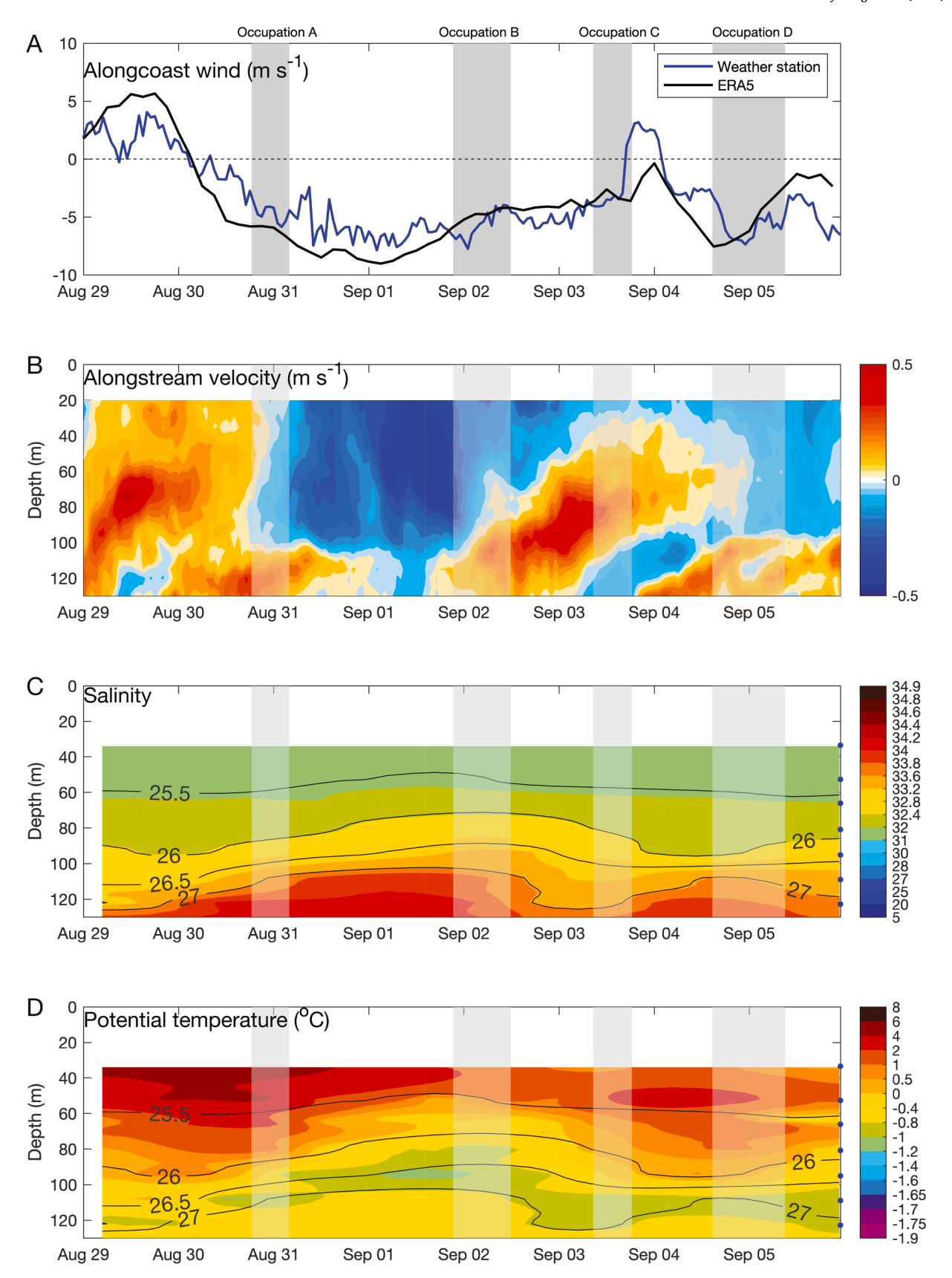


Fig. 2. Timeseries of the upwelling event. (A) The alongcoast wind speed from the Utqiagvik weather station and the ERA5 reanalysis. Negative values correspond to winds from the east. The gray bars denote the time periods of the four ship transects occupations. (B) Alongstream velocity, where positive is to the east. (C) Salinity (color) overlain by potential density (contours, kg m $^{-3}$). The blue dots denote the locations of the MicroCATs on the mooring. (D) Same as (C) except for potential temperature (color, $^{\circ}$ C).

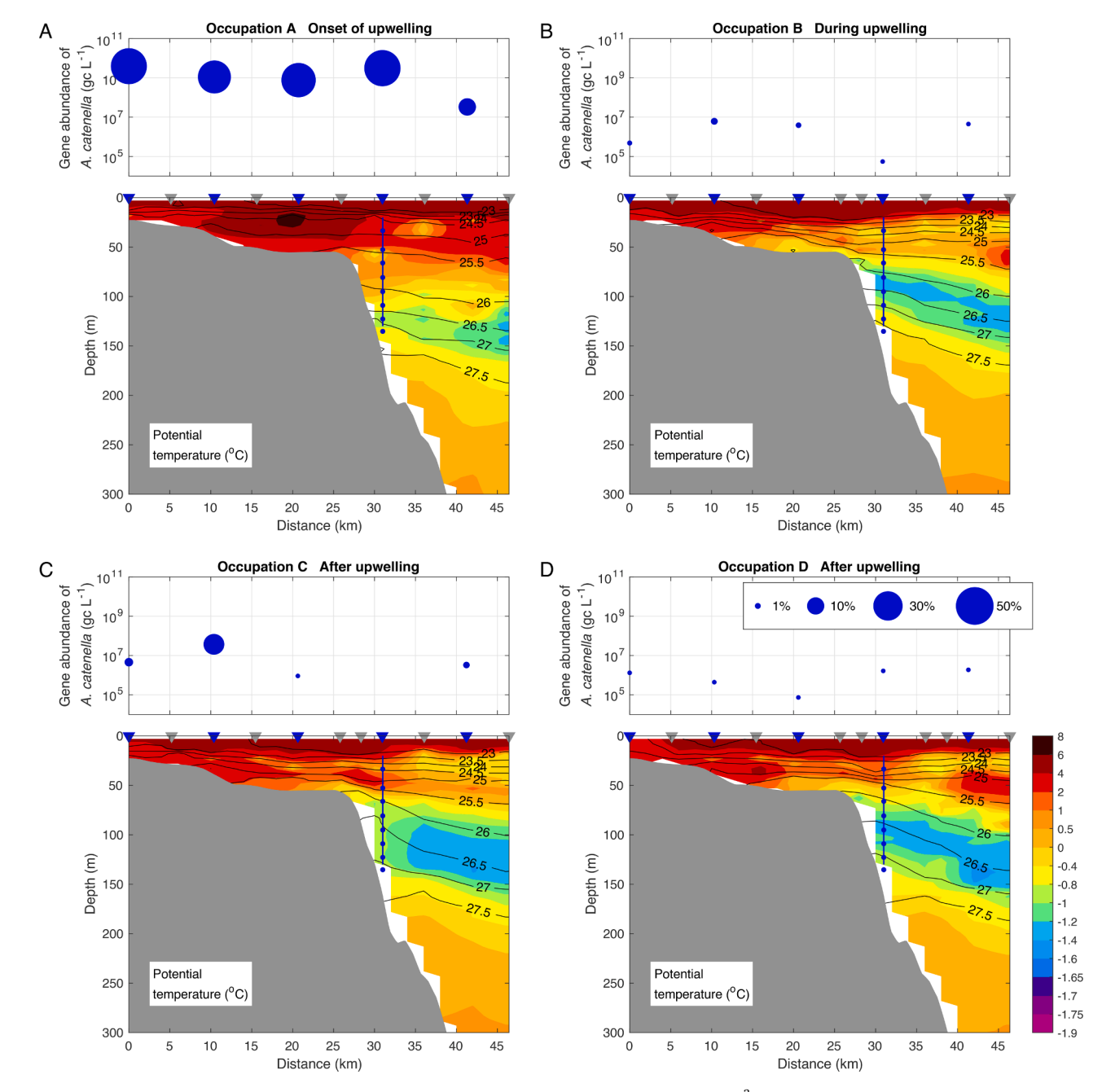


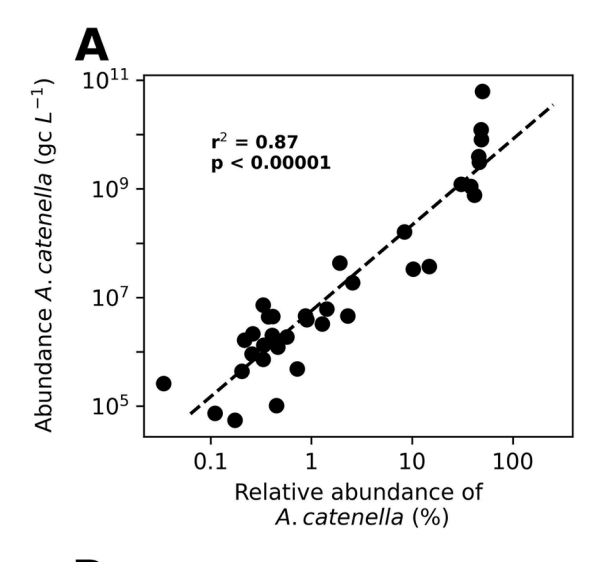
Fig. 3. Vertical sections of potential temperature (color, °C)) overlain by potential density (contours, kg m⁻³) for (A) onset of upwelling, (B) during upwelling, and (C, D) after upwelling. Station locations indicated by triangles across the top of the section with blue triangles indicating those at which surface water was collected. While the AON mooring is not on the transect, the location of the mooring with respect to the shelf on the sampled transect is plotted as a blue line for reference with dots indicating the locations of MicroCATs along the mooring profile. The corresponding concentrations of absolute *A. catenella* 28S rRNA gene abundance from surface collected samples are plotted above the sections, with the relative fraction of *A. catenella* 18S rRNA of total eukaryotic phytoplankton (dinoflagellates, diatoms, haptophytes) 18S rRNA indicated by the symbol size. Thresholds that were imaged by FlowCAM were 28S rRNA gene abundance of > 3.92E+09 gc L⁻¹ and a relative *A. catenella* 18S rRNA abundance of the total phytoplankton community of > 45%.

Table 1 P-values from Dunn's post hoc test comparing differences in 28S rRNA absolute gene abundance of *A. catenella* sequencing reads in shelf samples (surface and chl-*a*) between occupations of the transect. ns – not significant.

	Α	В	С	D
Α	_			
В	0.022	-		
C	0.020	ns	-	
D	0.005	ns	ns	-

Table 2 P-values from Dunn's post hoc test comparing differences in 18S rRNA relative abundance of *A. catenella* sequencing reads in shelf samples (surface and chl-*a*) between occupations of the transect. ns – not significant.

	A	В	C	D
A	_			
В	0.043	-		
C	0.0015	ns	-	
D	< 0.0001	ns	0.040	_



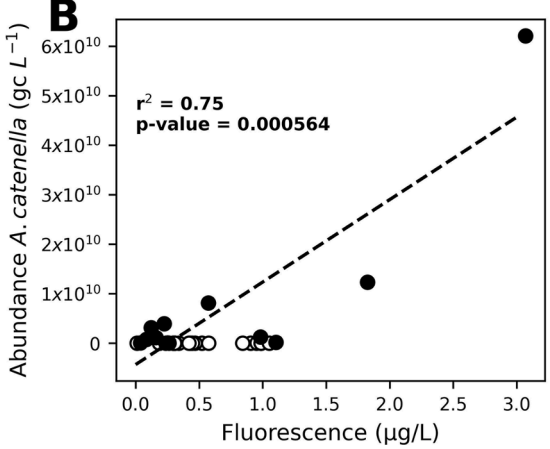


Fig. 4. Observed relationships between *A. tamarense* 28S gene abundance and other measured variables. A) Relationship between relative *A. catenella* 18S rRNA as a fraction of total eukaryotic phytoplankton (dinoflagellates, diatoms, haptophytes) 18S rRNA and absolute *A. catenella* 28S rRNA gene abundance; both are on a log scale. B) Relationship plotted between fluorescence and absolute 28S rRNA gene abundance of *A. catenella*; not on a log scale. Samples that had a relative abundance of *A. catenella* above 5% (from 18S analysis) are solid black circles and samples that had a relative abundance below 5% are empty black circles.

 $27.5~kg~m^{-3}$ isopycnals were at their shallowest depth during occupation B, consistent with the AON mooring data indicating that this was near the height of the upwelling.

4.2. A. catenella presence on the Beaufort shelf

This study confirms the presence and abundance of *Alexandrium* – specifically the species A. catenella – on the Alaskan Beaufort Sea shelf using imaging, sequencing, and qPCR methods. It is known that dinoflagellates have higher gene copy numbers than other unicellular eukaryotes (Cusick and Sayler, 2013; Lin, 2011), thus there is some concern when using ribosomal gene abundance to analyze eukaryotic community composition due to this copy number variability. However, we are encouraged that when Alexandrium was imaged by FlowCAM in a sample (n = 5), it corresponded with the five highest samples in terms of A. catenella 18S rRNA relative abundance of phytoplankton sequences, and the five highest absolute 28S rRNA gene abundances of A. catenella. Furthermore, our combined approach found that as the relative abundance of A. catenella, as a proportion of phytoplankton sequences, increased, the absolute gene abundance of A. catenella in our samples

increased. Based on our results, the thresholds for visualization on the FlowCAM were > 3.92E+09 gc L $^{-1}$ for 28S rRNA gene abundance, which was associated with >45% relative abundance of A. catenella in total 18S rRNA reads. Even though we found the three methods of measuring A. catenella abundance to corroborate with each other, because of known issues with variability in ribosomal gene abundance discussed above and the small size of our dataset, we caution against using this value as a hard threshold. We are encouraged, however, that with further sampling of A. catenella using these methods it may be possible to determine with more certainty the threshold at which A. catenella is imaged on the FlowCAM. A loftier but potentially achievable goal would be to further determine a threshold associated with toxic blooms. This would potentially allow for the use of imaging equipment like FlowCAM to analyze samples collected from remote areas for monitoring.

Previous work has estimated that the average number of 18S rRNA copies per cell of A. catenella is 46,000 (Yarimizu et al., 2021). If we use this value to convert our results into cell densities, the threshold density to be imaged on the FlowCAM was 67,000 cells L^{-1} , which is an order of magnitude higher than 1000 cells L^{-1} found to be the level at which A. catenella can pose a health risk (Jester et al., 2009). We acknowledge that A. catenella 28S rRNA sequence counts may be overestimated using this approach due to the qPCR standard curve method used (Hou et al., 2010) and known variability in ribosomal copy numbers per cell depending on the strain (Yarimizu et al., 2021). In addition, without knowing the level of toxin in these samples it is unsure whether the abundance of A. catenella were at levels that could pose a health risk. That said, the three methods we used validate each other and may indicate that the cell densities of A. catenella were at problematic levels before upwelling was at its peak.

4.3. A. catenella upwelling response

The results show that the absolute and relative abundances of *A. catenella* were statistically different at the onset of the upwelling event (occupation A) versus during/after the event (occupations B, C, and D). More specifically, our qPCR results show ~2 orders of magnitude higher *A. catenella* on the shelf and in the vicinity of the shelfbreak at the onset of the upwelling event when compared to samples collected during and after the event. The same pattern was seen in the 18S rRNA relative gene abundance of *A. catenella*, where it accounted for >40% of the eukaryotic phytoplankton sequencing reads at the start of upwelling and decreased to <1% after the upwelling. There was one exception to these general patterns on the shelf, which is that slightly higher relative abundance of 18S rRNA and absolute abundance of 28S rRNA were detected in the surface sample collected at the onshore start of the transect after upwelling (occupation C).

It is widely understood that an increase in nutrients in the euphotic zone should lead to higher algal biomass (Cushing, 1971; Iles et al., 2012; Jackson et al., 2011; Loubere, 2000; Tenore et al., 1995), but the abundance of A. catenella dramatically dropped during the upwelling when increased nitrate concentrations were found on the Alaskan Beaufort Sea shelf. This is consistent with evidence that dinoflagellates often dominate the phytoplankton community during lag phases between upwelling events, after diatoms have responded to the increase in nutrients (Lewitus et al., 2012). Alexandrium is thought to initiate blooms offshore and accumulate in coastal areas only after upwelling favorable winds subside (Anderson et al., 2008). Nitrate profile data from the calibrated SUNA sensor enabled us to confirm that nitrate upwelling occurred with the shallowing of the isopycnals associated with wind shifts. It is reasonable to assume that additional nutrient concentrations also increased with upwelling based on previous work in the area (Eddy et al., 2004; Mundy et al., 2009). However, as additional nutrients such as silicic acid and phosphate were only measured on a handful of samples from the broader cruise, we are unable to comment on whether species distributions changes could have been associated

with specific shifts in macronutrient ratios (i.e., between nitrate, phosphate, silicic acid ratios) or simply as a result of the arrival of elevated nutrients as a whole.

These results are supportive of our hypothesis that the Alexandrium population present in our study site at the onset of upwelling had been transported there by the eastward-flowing Beaufort shelfbreak jet. This hypothesis is also consistent with previous data collected 105 km west of our study site where high levels of Alexandrium were measured on a transect just east of Barrow Canyon occupied in August 2018-2019 (Anderson et al., 2021a). In that study the cells were found in the warm Alaskan Coastal Water and sea-ice melt water being advected eastward in the Beaufort shelfbreak jet and it was suggested that the cells may have entered the water column from a local seed bed just east of the canyon (Anderson et al., 2021a). At the time, the Barrow Canyon was the furthest east that Alexandrium had been observed along the northern Alaskan coast. Our work indicates that the proliferation of *Alexandrium* by the Beaufort shelfbreak jet continues east much further than Barrow Canyon. Further evidence that the Beaufort shelfbreak jet is the main conduit for Alexandrium proliferation into the Beaufort Sea is that the sample from the upper slope (~41 km from the onshore end of the transect and further offshore than the Beaufort shelfbreak jet) showed only slightly enhanced levels of *Alexandrium* at the onset of upwelling. Additionally, test station samples collected at the start of the expedition in the center of the Beaufort shelfbreak jet had similarly high A. catenella gene counts as those observed in our main transect at the onset of upwelling. The absence of both the Alaskan Coastal Water and the Alexandrium signal during occupations B, C, and D is likely due to the reversed Beaufort shelfbreak jet having advected them back to the west. Additionally, the secondary circulation during the upwelling event would tend to transport material offshore in the surface Ekman layer (Schulze and Pickart, 2012), which, together with enhanced wind mixing during upwelling (Spall, 2004), could significantly reduce the surface signature of Alexandrium on the shelf.

4.4. A comment on numerical abundances of A. catenella

While our results found that the relative abundance of A. catenella at times accounted for up to 45% of the phytoplankton 18S rRNA reads, it is important to note that this likely reflects higher ribosomal gene counts found in dinoflagellates compared with other phytoplankton (Gong and Marchetti, 2019; Lin, 2011). In other words, it would likely be an overestimation to state that A. catenella comprised 45% of the phytoplankton community at this time. That said, in samples collected at the onset of upwelling (and all samples where A. catenella accounted for >% 5 of the 18S rRNA reads), fluorescence had a significant positive relationship with A. catenella absolute gene abundance. Thus, while A. catenella may not have accounted for 45% of the phytoplankton community, we can infer that it was likely an important part of the phytoplankton biomass at the onset of the upwelling. We acknowledge that the outlier in the top right corner of Fig. 4B appears to skew the regression analysis. This potential outlier was sampled at the chlorophyll max depth (depth at which fluorescence was highest) at the Test Station (Fig. 1), which was located roughly in the middle of the shelfbreak jet before any upwelling had occurred. Both the surface and chlorophyll max samples from this station were included in this visualization and analysis to further analyze the contribution A. catenella had to the relative phytoplankton community. With the limited number of samples, we did not want to exclude any available data points. Removing the possible outlier point changes the absolute value of the regression and we caution that the intent of this figure is not to quantify a relationship between $gc L^{-1}$ of A. catenella and fluorescence. The point of the exercise was to confirm that when the relative abundance of A. catenella 18S sequences accounted for a significant percentage of the phytoplankton community 18S sequences, there was a corresponding increase in both 28S absolute gene abundance of A. catenella and fluorescence, indicating that A. catenella was a dominant component of the phytoplankton community in these samples. During and after the upwelling no such relationship is seen between *A. catenella* gene abundance and fluorescence, no *Alexandrium* images were observed by the FlowCAM, and there was low relative abundance of *A. catenella* 18S rRNA reads. This suggests that, as the Beaufort shelfbreak jet reversed during upwelling, the *A. catenella* population decreased and it was no longer a dominant phytoplankton in the region.

4.5. Future monitoring

A. catenella is one of the species of the Alexandrium genus that forms resting cysts as a part of their life cycle, and Alexandrium cysts are known to have an internal clock to bloom when suitable conditions exist (Anderson et al., 2014). A. catenella cysts have been found in temperature ranges from -0.6 to 26.8 °C, with the highest abundances found between 5 and 15 °C (Marret and Zonneveld, 2003). The surface temperature on the shelf at the onset of the upwelling event was > 5 °C. As Alexandrium has the ability to produce resting cysts to survive and take advantage of suitable conditions (Anderson et al., 2014; Brosnahan et al., 2017; Wall, 1971), it may be important to monitor this area for future Alexandrium blooms and further expansion associated with the Beaufort shelfbreak jet. Future monitoring may be especially important considering that A. catenella has been observed in the California Current upwelling system as an opportunistic dinoflagellate that can germinate in a variety of conditions, including upwelling (Pitcher et al., 2017), although our data did not show evidence of Alexandrium associated with Arctic upwelling. The region of the shelf where A. catenella was observed is relatively shallow (~21 m to 56 m), thus strong storms that lead to mixing events on the shelf, could resuspend Alexandrium cysts and possibly lead to a bloom. While upwelling was seen to cause a sharp drop in the abundance of A. catenella in our study, presumably the mixing caused by upwelling could also cause a reintroduction of A. catenella cysts to the water column, which may lead to the germination and proliferation of the cells as upwelling relaxes and warm Beaufort shelfbreak jet water begins to flow on the shelf again. While in our study two competing factors were documented to influence Alexandrium abundance, the Beaufort shelfbreak jet and upwelling/reversal of the Beaufort shelfbreak jet, another factor to consider is the resuspension of A. catenella cysts and subsequent germination during suitable periods between upwelling events. As was documented by Anderson et al. (2021a) a large cyst bed of A. catenella is located on the shelf west of our sampling site. This reinforces that more study is needed to accurately document abundance and toxicity throughout this region, as the factors influencing A. catenella abundance indicate likely prevalence and further dispersion of the HAB with periods of decreased abundance during upwelling. Additional sampling in this area that includes analysis of nutrients, targeted toxin testing, cell imaging, and sequencing analysis at a higher resolution covering a time period fully encompassing upwelling, relaxation, and standard flow of the Beaufort shelfbreak jet, will likely allow for a stronger foundation to correlate A. catenella abundance with non-upwelling and upwelling events. Importantly, these results can be added to harmful algal bloom modeling efforts to predict future occurrences of toxic levels of A. catenella.

While not all species or even strains of *Alexandrium* produce saxitoxin (Anderson et al., 2012), there have been documented cases of *Alexandrium* blooms, and saxitoxin bioaccumulation, seen along the Alaskan coast up to and just east of Point Barrow (Lefebvre et al., 2016). Presumably, these events were the result of the Alaskan Coastal Current bringing warm water suitable for *Alexandrium* populations to thrive and they produced saxitoxin that eventually led to marine mammal deaths. It has been noted that *Alexandrium* may produce saxitoxin as a pheromone or as an indicator of cyst settlement (Wyatt and Jenkinson, 1997); thus, if an *Alexandrium* bloom is observed in this area, saxitoxin and any further bioaccumulation will need to be monitored closely. Due to the previously documented bioaccumulation of saxitoxin seen along the coast of Alaska up to Point Barrow (Lefebvre et al., 2016), we can

hypothesize that this proliferation will continue along the Alaskan Beaufort Sea coast because of delivery by the warming Beaufort shelf-break jet, the warming Arctic as a whole, and the potential for transport from the cyst beds of *Alexandrium* west of our study site. This proliferation is a concern as fish, sea birds, and mammals, including bowhead and beluga whales, are known to spawn in this region primarily due upwelling events that cause increased primary production and zooplankton proliferation (Ashjian et al., 2010). Any proliferation of a potential toxin-producing organism that can impact upper trophic levels in the region would be especially consequential to the Inuvialuit, indigenous people in the western Canadian Arctic, who depend on this ecosystem (Ayles et al., 2016).

Finding A. catenella this far east on the Alaskan Beaufort Sea shelf indicates that the Beaufort shelfbreak jet continues transporting warm water suitable for Alexandrium population expansion well past Barrow Canyon. It should also be noted that strong westerly winds are common in this region during summer, which accelerate the Beaufort shelfbreak jet and lead to downwelling (Foukal et al., 2019). This is notable, as it is similar to an anomaly that aligned with an A. catenella (referred to as A. fundyense in cited study) bloom in the Gulf of Maine where downwelling favorable winds were thought to have caused a coastal accumulation of Alexandrium (McGillicuddy et al., 2014). Easterly winds in the Alaskan Beaufort Sea intensify in the fall, and upwelling activity increases (Lin et al., 2016; Pickart et al., 2013). This tends to slow the Beaufort shelfbreak jet, flux warm surface water offshore, and upwell colder water from the basin. Indeed, Bering Summer Water replaced much of the Alaskan Coastal Water over the outer shelf on occupations B-D. This upwelled water was several degrees colder, changing the environmental conditions away from those likely suitable for Alexandrium. These results lead us to suspect that if A. catenella were to bloom, it would occur earlier in the Arctic summer when the Beaufort shelfbreak jet advects warm water to the Beaufort Sea and is not subject to as much upwelling. It is worth noting, however, that there are evolutionary adaptations in Alexandrium species that could allow for survival during upwelling, such as temporary chain formations and shifts in swimming velocity to adjust to turbulence (Smayda and Trainer, 2010). These evolutionary advantages suggest that increased upwelling alone may not deter Alexandrium from surviving on the Alaskan Beaufort Sea shelf.

5. Conclusion

Heat transport by currents into the Arctic is predicted to continue increasing (Marshall et al., 2014, 2015) presumably resulting in the Beaufort shelf continuing to warm. Higher temperatures in coastal waters have been determined to cause the accumulation of *A. catenella* in the Gulf of Maine (He and McGillicuddy, 2008), and with the likely warming of the Beaufort Sea shelf, we can predict that the same may occur here. However, since upwelling along the Beaufort Sea shelf is predicted to increase as well (Pickart et al., 2013), there are competing forces at play that could influence *Alexandrium* proliferation in the region. Either way, it is prudent to further evaluate this area for *A. catenella* cell densities, toxin production and determine the extent to which the Beaufort shelfbreak jet and upwelling influence levels of *A. catenella*.

Declaration of Competing Interest

The authors declare no competing interests.

Data availability

Sample and station information, including qPCR results, and nitrate profiles are hosted at Arctic Data Center (https://arcticdata.io/catalog/view/doi%3A10.18739%2FA2K649T9V). Cruise CTD files can be found on R2R (https://www.rvdata.us/; Cruise ID: SKQ201713S) Raw sequence files can be accessed via NCBI SRA (https://www.ncbi.nlm.

nih.gov/sra; BioProject ID: PRJNA743005). FlowCAM images can be found on Ecotaxa (https://ecotaxa.obs-vlfr.fr/; Project ID: skq201713s).

Acknowledgments

We thank the captain, crew, and marine science technicians of R/V *Sikuliaq* for facilitating sample collection, Kim Powell (Old Dominion University) for assisting in DNA/RNA sample processing, and Steve Okkonen (University of Alaska Fairbanks) for help determining the physical dynamics of the upwelling event, Amala Mahadevan (Woods Hole Oceanographic Institution) for the use of her SUNA V2 nitrate sensor, and Laurie Juranek (Oregon State University) for analyzing the nitrate samples that we collected. Funding for this work was provided by awards from the Jeffress Trust Awards Program in Interdisciplinary Research to PDC, the Jacques S. Zaneveld endowed scholarship to SVE, and the Weston Howland Jr. Postdoctoral Scholarship and WHOI Access to Sea Fund to KL. Fieldwork was supported in part by National Science Foundation (NSF) grant PLR-1603941 (CA). A portion of the analysis was funded by NSF grant OPP-1733564 and National Oceanic and Atmospheric Administration grant NA14OAR4320158 (PL and RP).

Supplementary materials

Supplementary material associated with this article can be found, in the online version, at doi:10.1016/j.hal.2022.102346.

References

- Altschul, S.F., Gish, W., Miller, W., Myers, E.W., Lipman, D.J., 1990. Basic local alignment search tool. J. Mol. Biol. 215 (3), 403–410. https://doi.org/10.1016/
- Anderson, D.M., Alpermann, T.J., Cembella, A.D., Collos, Y., Masseret, E., Montresor, M., 2012. The globally distributed genus Alexandrium: multifaceted roles in marine ecosystems and impacts on human health. Harmful Algae 14, 10–35. https://doi. org/10.1016/j.hal.2011.10.012.
- Anderson, D.M., Burkholder, J.M., Cochlan, W.P., Glibert, P.M., Gobler, C.J., Heil, C.A., Kudela, R.M., Parsons, M.L., Rensel, J.E.J., Townsend, D.W., Trainer, V.L., Vargo, G. A., 2008. Harmful algal blooms and eutrophication: examining linkages from selected coastal regions of the United States. Harmful Algae 8 (1), 39–53. https://doi.org/10.1016/j.hal.2008.08.017.
- Anderson, D.M., Fachon, E., Pickart, R.S., Lin, P., Fischer, A.D., Richlen, M.L., Uva, V., Brosnahan, M.L., McRaven, L., Bahr, F., Lefebvre, K., Grebmeier, J.M., Danielson, S. L., Lyu, Y., Fukai, Y., 2021a. Evidence for massive and recurrent toxic blooms of Alexandrium catenella in the Alaskan Arctic. PNAS 118 (41), e2107387118. https://doi.org/10.1073/pnas.2107387118.
- Anderson, D.M., Fensin, E., Gobler, C.J., Hoeglund, A.E., Hubbard, K.A., Kulis, D.M., Landsberg, J.H., Lefebvre, K.A., Provoost, P., Richlen, M.L., Smith, J.L., Solow, A.R., Trainer, V.L., 2021b. Marine harmful algal blooms (HABs) in the United States: history, current status and future trends. Harmful Algae 102, 101975. https://doi. org/10.1016/j.hal.2021.101975.
- Anderson, D.M., Keafer, B.A., Kleindinst, J.L., McGillicuddy, D.J., Martin, J.L., Norton, K., Pilskaln, C.H., Smith, J.L., Sherwood, C.R., Butman, B., 2014.
 Alexandrium fundyense cysts in the gulf of maine: long-term time series of abundance and distribution, and linkages to past and future blooms. Deep-Sea Res. Pt. II 103, 6–26. https://doi.org/10.1016/j.dsr2.2013.10.002.
- Ashjian, C.J., Braund, S.R., Campbell, R.G., George, J.C.C., Kruse, J., Maslowski, W., Moore, S.E., Nicolson, C.R., Okkonen, S.R., Sherr, B.F., Sherr, E.B., Spitz, Y.H., 2010. Climate variability, oceanography, bowhead whale distribution, and inupiat subsistence whaling near barrow, Alaska. Arctic 63 (2), 179–194. https://doi.org/10.14430/arctic973.
- Ayles, B., Porta, L., Clarke, R.M., 2016. Development of an integrated fisheries comanagement framework for new and emerging commercial fisheries in the Canadian Beaufort Sea. Mar. Policy 72, 246–254. https://doi.org/10.1016/j. marpol.2016.04.032.
- Biller, D.V., Coale, T.H., Till, R.C., Smith, G.J., Bruland, K.W., 2013. Coastal iron and nitrate distributions during the spring and summer upwelling season in the central California Current upwelling regime. Cont. Shelf. Res. 66, 58–72. https://doi.org/ 10.1016/j.csr.2013.07.003.
- Brosnahan, M.L., Ralston, D.K., Fischer, A.D., Solow, A.R., Anderson, D.M., 2017. Bloom termination of the toxic dinoflagellate Alexandrium catenella: vertical migration behavior, sediment infiltration, and benthic cyst yield. Limnol. Oceanogr. 62 (6), 2829–2849. https://doi.org/10.1002/lno.10664.
- Callahan, B.J., McMurdie, P.J., Rosen, M.J., Han, A.W., Johnson, A.J.A., Holmes, S.P., 2016. DADA2: high-resolution sample inference from Illumina amplicon data. Nat. Methods 13 (7), 581–583. https://doi.org/10.1038/nmeth.3869.

Cushing, D.H., 1971. Upwelling and the production of fish. Adv. Mar. Biol. 9, 255–334. https://doi.org/10.1016/S0065-2881(08)60344-2.

- Cusick, K.D., Sayler, G.S., 2013. An overview on the marine neurotoxin, saxitoxin: genetics, molecular targets, methods of detection and ecological functions. Mar. Drugs 11 (4), 991–1018. https://doi.org/10.3390/md11040991.
- Eddy, C.C., Robie, W.M., Steve, J., 2004. Phytoplankton productivity on the Canadian Shelf of the Beaufort Sea. Mar. Ecol. Prog. Ser. 277, 37–50. https://doi.org/10.3354/ meps277037.
- Foukal, N.P., Pickart, R.S., Moore, G.W.K., Lin, P., 2019. Shelfbreak downwelling in the Alaskan Beaufort Sea. J. Geophys. Res-Oceans 124 (10), 7201–7225. https://doi. org/10.1029/2019JC015520.
- Fraga, S., Sampedro, N., Larsen, J., Moestrup, Ø., Calado, A.J., 2015. Arguments against the proposal 2302 by John & al. to reject the name Gonyaulax catenella (Alexandrium catenella). Taxon 64 (3), 634–635. https://doi.org/10.12705/643.15.
- Gloor, G.B., Macklaim, J.M., Pawlowsky-Glahn, V., Egozcue, J.J., 2017. Microbiome datasets are compositional: and this is not optional. Front. Microbiol. 8 https://doi. org/10.3389/fmicb.2017.02224.
- Gong, W., Marchetti, A., 2019. Estimation of 18S gene copy number in marine eukaryotic plankton using a next-generation sequencing approach. Front. Mar. Sci. 6 (219) https://doi.org/10.3389/fmars.2019.00219.
- Gordon, L.I., Jennings Jr., J.C., Ross, A.A., Krest, J.M., 1993. A suggested protocol for continuous flow automated analysis of seawater nutrients (phosphate, nitrate, nitrite and silicic acid) in the WOCE hydrographic program and the joint global ocean fluxes study. WOCE Hydrogr. Progr. Off., Methods Manual WHPO (68/91), 1–52.
- Grattan, L.M., Holobaugh, S., Morris, J.G., 2016. Harmful algal blooms and public health. Harmful Algae 57, 2–8. https://doi.org/10.1016/j.hal.2016.05.003.
- Hallegraeff, G., Enevoldsen, H., Zingone, A., 2021. Global harmful algal bloom status reporting. Harmful Algae 102 (101992). https://doi.org/10.1016/j. bal. 2021.101992
- He, R., McGillicuddy Jr, D.J., 2008. Historic 2005 toxic bloom of Alexandrium fundyense in the west Gulf of Maine: 1. In situ observations of coastal hydrography and circulation. J. Geophys. Res-Oceans 113 (C7). https://doi.org/10.1029/ 2007JC004601.
- Hersbach, H., Rosnay, P., Schepers, D., Simmons, A., Soci, C., Abdalla, S., Alonso, M.,
 Balmaseda, Balsamo, G., Bechtold, P., Berrisford, P., Bidlot, J., Boisséson, E.D.,
 Bonavita, Browne, P., Diamantakis, M., 2018. Operational Global Reanalysis:
 Progress, Future Directions and Synergies With NWP. ERA Report Series, Reading.
- Holland, M.M., Bitz, C.M., 2003. Polar amplification of climate change in coupled models. Clim. Dynam. 21 (3), 221–232. https://doi.org/10.1007/s00382-003-0332-6
- Hosoi-Tanabe, S., Sako, Y., 2005. Species-specific detection and quantification of toxic marine dinoflagellates Alexandrium tamarense and A. catenella by Real-time PCR assay. Mar. Biotechnol. 7 (5), 506–514. https://doi.org/10.1007/s10126-004-4128-
- Hou, Y., Zhang, H., Miranda, L., Lin, S., 2010. Serious Overestimation in quantitative PCR by circular (Supercoiled) Plasmid standard: microalgal pcna as the model gene. PLoS One 5 (3), e9545. https://doi.org/10.1371/journal.pone.0009545.
- Iles, A.C., Gouhier, T.C., Menge, B.A., Stewart, J.S., Haupt, A.J., Lynch, M.C., 2012. Climate-driven trends and ecological implications of event-scale upwelling in the California current system. Glob. Change Biol. 18 (2), 783–796. https://doi.org/ 10.1111/j.1365-2486.2011.02567.x.
- Jackson, T., Bouman, H.A., Sathyendranath, S., Devred, E., 2011. Regional-scale changes in diatom distribution in the Humboldt upwelling system as revealed by remote sensing: implications for fisheries. ICES J. Mar. Sci. 68 (4), 729–736. https://doi. org/10.1093/icesims/fsq181.
- Jester, R., Lefebvre, K., Langlois, G., Vigilant, V., Baugh, K., Silver, M.W., 2009. A shift in the dominant toxin-producing algal species in central California alters phycotoxins in food webs. Harmful Algae 8 (2), 291–298. https://doi.org/10.1016/j. bal.2008.07.001
- John, U., Litaker, R.W., Montresor, M., Murray, S., Brosnahan, M.L., Anderson, D.M., 2014. Formal revision of the Alexandrium tamarense species complex (Dinophyceae) taxonomy: the introduction of five species with emphasis on molecular-based (rDNA) classification. Protist 165 (6), 779–804. https://doi.org/10.1016/j. protis.2014.10.001.
- Kim, K.Y., Hamlington, B.D., Na, H., Kim, J., 2016. Mechanism of seasonal arctic sea ice evolution and arctic amplification. Cryosphere 10 (5), 2191–2202. https://doi.org/ 10.5194/tc-10-2191-2016
- Kruskal, W.H., Wallis, W.A., 1952. Use of ranks in one-criterion variance analysis. J. Am. Stat. Assoc. 47 (260), 583–621. https://doi.org/10.1080/ 01621459.1952.10483441.
- Lefebvre, K.A., Quakenbush, L., Frame, E., Huntington, K.B., Sheffield, G., Stimmelmayr, R., Bryan, A., Kendrick, P., Ziel, H., Goldstein, T., Snyder, J.A., Gelatt, T., Gulland, F., Dickerson, B., Gill, V., 2016. Prevalence of algal toxins in Alaskan marine mammals foraging in a changing arctic and subarctic environment. Harmful Algae 55, 13–24. https://doi.org/10.1016/j.hal.2016.01.007.
- Lewitus, A.J., Horner, R.A., Caron, D.A., Garcia-Mendoza, E., Hickey, B.M., Hunter, M., Huppert, D.D., Kudela, R.M., Langlois, G.W., Largier, J.L., Lessard, E.J., RaLonde, R., Jack Rensel, J.E., Strutton, P.G., Trainer, V.L., Tweddle, J.F., 2012. Harmful algal blooms along the North American west coast region: history, trends, causes, and impacts. Harmful Algae 19, 133–159. https://doi.org/10.1016/j.hal.2012.06.009.
- Lilly, E.L., Halanych, K.M., Anderson, D.M., 2007. Species boundaries and global biogeography of the Alexandrium tamarense complex (Dinophyceae)1. J. Phycol. 43 (6), 1329–1338. https://doi.org/10.1111/j.1529-8817.2007.00420.x.
- Lin, P., Pickart, R.S., Moore, G.W.K., Spall, M.A., Hu, J., 2019. Characteristics and dynamics of wind-driven upwelling in the Alaskan Beaufort Sea based on six years of

- mooring data. Deep-Sea Res. Pt. II 162, 79–92. https://doi.org/10.1016/j.dsr2.2018.01.002
- Lin, P., Pickart, R.S., Stafford, K.M., Moore, G.W.K., Torres, D.J., Bahr, F., Hu, J., 2016. Seasonal variation of the Beaufort shelfbreak jet and its relationship to Arctic cetacean occurrence. J. Geophys. Res-Oceans 121 (12), 8434–8454. https://doi.org/ 10.1002/2016JC011890.
- Lin, S., 2011. Genomic understanding of dinoflagellates. Res. Microbiol. 162 (6), 551–569. https://doi.org/10.1016/j.resmic.2011.04.006.
- Loubere, P., 2000. Marine control of biological production in the eastern equatorial Pacific Ocean. Nature 406 (6795), 497–500. https://doi.org/10.1038/35020041.
- Manabe, S., Stouffer, R.J., 1980. Sensitivity of a global climate model to an increase of CO2 concentration in the atmosphere. J. Geophys. Res-Oceans 85 (C10), 5529–5554. https://doi.org/10.1029/JC085iC10p05529.
- Marret, F., Zonneveld, K.A.F., 2003. Atlas of modern organic-walled dinoflagellate cyst distribution. Rev. Palaeobot. Palynol. 125 (1), 1–200. https://doi.org/10.1016/ S0034-6667(02)00229-4
- Marshall, J., Armour, K.C., Scott, J.R., Kostov, Y., Hausmann, U., Ferreira, D., Shepherd, T.G., Bitz, C.M., 2014. The ocean's role in polar climate change: asymmetric Arctic and Antarctic responses to greenhouse gas and ozone forcing. Philos. Trans. R. Soc. A 372 (2019), 20130040. https://doi.org/10.1098/rsta.2013.0040
- Marshall, J., Scott, J.R., Armour, K.C., Campin, J.M., Kelley, M., Romanou, A., 2015. The ocean's role in the transient response of climate to abrupt greenhouse gas forcing. Clim. Dynam. 44 (7), 2287–2299. https://doi.org/10.1007/s00382-014-2308-0.
- McGillicuddy, D.J., Brosnahan, M.L., Couture, D.A., He, R., Keafer, B.A., Manning, J.P., Martin, J.L., Pilskaln, C.H., Townsend, D.W., Anderson, D.M., 2014. A red tide of Alexandrium fundyense in the Gulf of Maine. Deep-Sea Res. Pt. II 103, 174–184. https://doi.org/10.1016/j.dsr2.2013.05.011.
- Mundy, C.J., Gosselin, M., Ehn, J., Gratton, Y., Rossnagel, A., Barber, D.G., Martin, J., Tremblay, J.-É., Palmer, M., Arrigo, K.R., Darnis, G., Fortier, L., Else, B., Papakyriakou, T., 2009. Contribution of under-ice primary production to an ice-edge upwelling phytoplankton bloom in the Canadian Beaufort Sea. Geophys. Res. Lett. 36 (17) https://doi.org/10.1029/2009GL038837.
- Natsuike, M., Matsuno, K., Hirawake, T., Yamaguchi, A., Nishino, S., Imai, I., 2017a. Possible spreading of toxic Alexandrium tamarense blooms on the Chukchi Sea shelf with the inflow of Pacific summer water due to climatic warming. Harmful Algae 61, 80–86. https://doi.org/10.1016/j.hal.2016.11.019.
- Natsuike, M., Nagai, S., Matsuno, K., Saito, R., Tsukazaki, C., Yamaguchi, A., Imai, I., 2013. Abundance and distribution of toxic Alexandrium tamarense resting cysts in the sediments of the Chukchi Sea and the eastern Bering Sea. Harmful Algae 27, 52–59. https://doi.org/10.1016/j.hal.2013.04.006.
- Natsuike, M., Oikawa, H., Matsuno, K., Yamaguchi, A., Imai, I., 2017b. The physiological adaptations and toxin profiles of the toxic Alexandrium fundyense on the eastern Bering Sea and Chukchi Sea shelves. Harmful Algae 63, 13–22. https://doi.org/10.1016/j.hal.2017.01.001.
- Nikolopoulos, A., Pickart, R.S., Fratantoni, P.S., Shimada, K., Torres, D.J., Jones, E.P., 2009. The western arctic boundary current at 152°W: structure, variability, and transport. Deep-Sea Res. Pt. II 56 (17), 1164–1181. https://doi.org/10.1016/j. dsr2.2008.10.014.
- Pickart, R.S., Moore, G.W.K., Torres, D.J., Fratantoni, P.S., Goldsmith, R.A., Yang, J., 2009. Upwelling on the continental slope of the Alaskan Beaufort Sea: storms, ice, and oceanographic response. J. Geophys. Res. Oceans 114 (C1). https://doi.org/ 10.1029/2008ic.005509
- Pickart, R.S., Spall, M.A., Mathis, J.T., 2013. Dynamics of upwelling in the Alaskan Beaufort Sea and associated shelf-basin fluxes. Deep-Sea Res. Pt. I 76, 35–51. https://doi.org/10.1016/j.dsr.2013.01.007.
- Pickart, R.S., Spall, M.A., Moore, G.W.K., Weingartner, T.J., Woodgate, R.A., Aagaard, K., Shimada, K., 2011. Upwelling in the Alaskan Beaufort Sea: atmospheric forcing and local versus non-local response. Prog. Oceanogr. 88 (1), 78–100. https:// doi.org/10.1016/j.pocean.2010.11.005.
- Pitcher, G.C., Jiménez, A.B., Kudela, R.M., Reguera, B., 2017. Harmful algal blooms in eastern boundary upwelling systems A GEOHAB CORE RESEARCH PROJECT. Oceanogr 30 (1), 22–35. https://doi.org/10.5670/oceanog.2017.107.
- Prud'homme van Reine, W.F., 2017. Report of the nomenclature committee for Algae: 16 on proposals to amend the code. Taxon 66 (1), 197–198. https://doi.org/10.12705/661.18.
- Schulze, L.M., Pickart, R.S., 2012. Seasonal variation of upwelling in the Alaskan Beaufort Sea: impact of sea ice cover. J. Geophys. Res. Oceans 117 (C6). https://doi. org/10.1029/2012JC007985.
- Smayda, T.J., Trainer, V.L., 2010. Dinoflagellate blooms in upwelling systems: seeding, variability, and contrasts with diatom bloom behaviour. Prog. Oceanogr. 85 (1), 92–107. https://doi.org/10.1016/j.pocean.2010.02.006.
- Spall, M.A., 2004. Boundary currents and watermass transformation in marginal seas. J. Phys. Oceanogr. 34 (5), 1197–1213. https://doi.org/10.1175/1520-0485(2004) 034<1197:BCAWTI>2.0.CO;2.
- Stoeck, T., Bass, D., Nebel, M., Christian, R., Jones, M.D.M., Breiner, H.W., Richards, T. A., 2010. Multiple marker parallel tag environmental DNA sequencing reveals a highly complex eukaryotic community in marine anoxic water. Mol. Ecol. 19 (s1), 21–31. https://doi.org/10.1111/j.1365-294X.2009.04480.x.
- Tenore, K.R., Alonso-Noval, M., Alvarez-Ossorio, M., Atkinson, L.P., Cabanas, J.M., Cal, R.M., Campos, H.J., Castillejo, F., Chesney, E.J., Gonzalez, N., Hanson, R.B., McClain, C.R., Miranda, A., Roman, M.R., Sanchez, J., Santiago, G., Valdes, L., Varela, M., Yoder, J., 1995. Fisheries and oceanography off Galicia, NW Spain: mesoscale spatial and temporal changes in physical processes and resultant patterns of biological productivity. J. Geophys. Res.-Oceans 100 (C6), 10943–10966. https://doi.org/10.1029/95JC00529.

- van der Linden, E.C., Le Bars, D., Bintanja, R., Hazeleger, W., 2019. Oceanic heat transport into the Arctic under high and low CO2 forcing. Clim. Dynam. 53 (7),
- 4763-4780. https://doi.org/10.1007/s00382-019-04824-y.
 Wall, D., 1971. Biological problems concerning fossilizable dinoflagellates. Proc. Ann. Meet. Am. Assoc. Stratigr. Palynol. 2, 1–15. https://doi.org/10.2307/3687273.
- Wang, D.Z., 2008. Neurotoxins from Marine Dinoflagellates: a brief review. Mar. Drugs 6
- (2), 349–371. https://doi.org/10.3390/md20080016. Woodgate, R.A., 2018. Increases in the pacific inflow to the Arctic from 1990 to 2015, and insights into seasonal trends and driving mechanisms from year-round Bering
- Strait mooring data. Prog. Oceanogr. 160, 124-154. https://doi.org/10.1016/j.
- Wyatt, T., Jenkinson, I.R., 1997. Notes on Alexandrium population dynamics. J. Plankton Res. 19 (5), 551–575. https://doi.org/10.1093/plankt/19.5.551.
 Yarimizu, K., Sildever, S., Hamamoto, Y., Tazawa, S., Oikawa, H., Yamaguchi, H.,
 - Basti, L., Mardones, J.I., Paredes-Mella, J., Nagai, S., 2021. Development of an absolute quantification method for ribosomal RNA gene copy numbers per eukaryotic single cell by digital PCR. Harmful Algae 103, 102008. https://doi.org/ 10.1016/j.hal.2021.102008.